JOURNAL OF MATERIALS SCIENCE 23 (1988) 3801–3815

# Review
# Synthetic and biological composites formed by *in situ* precipitation

PAUL CALVERT
*School of Chemistry, University of Sussex, Brighton BN1 9QJ, UK*
STEPHEN MANN
*School of Chemistry, University of Bath, Bath BA2 7AY, UK*

Filler particles are frequently put into polymers to improve the stiffness or strength. There are a number of other applications such as magnetic coatings and piezoelectric transducers where second phase particles are introduced to give the composite special properties. Many biological materials, including bone, are also composite with particles reinforcing a polymer matrix. In the preparation of the synthetic materials the filler is normally blended into the polymer. In the biological materials the particles are grown *in situ* within the polymeric matrix, and under the control of the matrix. Here we review the growth of particles when constrained by a polymeric matrix, both in natural and synthetic materials. We discuss the principles governing such processes and the potential for the production of highly structured composite materials by this route.

## 1. Introduction

Biological composite materials, such as bones, teeth and shells, have a polymeric matrix reinforced by a mineral, hydroxyapatite or calcium carbonate, which forms within the matrix. These materials are distinguished from any synthetic composites by their structural and organizational complexity. It seems reasonable that a group of similarly sophisticated artificial materials might be produced by precipitation within a polymer matrix although it might require a considerable effort of materials engineering. In this review we aim to describe studies of the production of composites by *in situ* precipitation within polymer matrices, and summarize the potential and constraints which apply to these materials as a group. The comparison is made between currently available synthetic materials and the characteristic types and organizational features of biological minerals, since an understanding of biogenic composites may provide important insight for future developments in materials technology.

Most biological materials are composites at all levels from the organization of individual macromolecules to the whole organism. Most of the materials which play a predominantly structural role comprise a swollen polymeric matrix reinforced with polymer fibres and/or with a mineral filler. In bone, for example, a glycosaminoglycan matrix is reinforced with collagen fibres and with ribbon- or plate-like crystallites of hydroxyapatite, a calcium phosphate. The extent of mineralization varies depending on the exact function of the bone and on the species. A typical level is about 38 vol % mineral with a crystallite thickness of 4 nm and lateral dimensions of 35 nm or more. The structure of mammalian tooth is similar but the mineral level is higher, about 86 vol %, and the individual crystallites are larger. Shells of invertebrates have a comparable range of structures but the mineral is normally calcium carbonate and the matrix is reinforced with chitin. In the context of synthetic composites, the biological materials have two striking characteristics. The shape, size, orientation and organization of the mineral in the matrix shows a high degree of sophistication (Fig. 1) when compared to the random dispersion of particles in a filled polymer composite; and the structures form by growth of the mineral phase in the polymer rather than by the synthetic route of dispersion of particles into a liquid resin.

The simplest way to prepare a precipitate within a polymer is to dissolve the additive in the polymer at high temperature and induce precipitation by cooling. This method will be limited to organophilic solutes, which have a high degree of solubility in the polymer. A more versatile method is to co-dissolve the additive and polymer in a mutual solvent which is then evaporated. A much wider range of composites can be prepared if precipitation is induced by a chemical reaction within the polymer. Bone mineralization could be viewed in this way in that calcium and phosphate are introduced into the matrix in a soluble form and then released to combine and precipitate. Mann [2] has recently reviewed the chemistry and physics of biological mineralization.

Precipitation within a polymer will differ from precipitation from solution in a number of ways. Firstly,

0022–2461/88 $03.00 + .12 

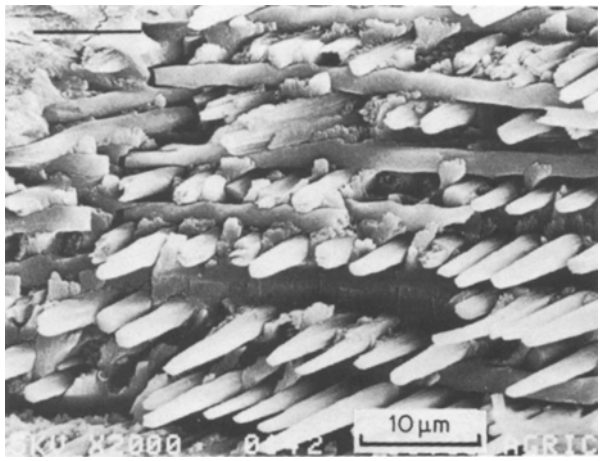


*Figure 1* Scanning electron micrograph of the enamel of late-maturing rat incisor showing two sets of coplanar rods in the plane of the micrograph and a perpendicular set of inter-rods. Each rod and inter-rod is composed of hundreds of elongated hydroxyapatite crystals, each of which is enveloped in a protein sheath or tubule. The crystals are fibrillar with the *c* axis parallel to the long axis which may be longer than 100 µm. (Reproduced with permission from Weiner [1]).

there is no convection or flow within a polymer so particle collisions and agglomeration will be largely eliminated. Particle growth will be controlled to a great extent by diffusive processes within the matrix. Also the matrix can be oriented and so can transmit a preferred orientation to the precipitate. In addition the matrix may be semicrystalline or otherwise structured such that there may be an epitaxial relationship between the polymer and the precipitate. In crystallization from solution the solvent can influence the particle morphology through the dependence of growth kinetics on the surface energy of different crystal faces. This effect would also be expected in polymeric media and may be the explanation for preferred precipitation sites in a number of precipitation-induced diseases such as gout. Finally, it is known that small concentrations of polymers in solution can modify or "poison" crystal growth by adsorption to surface step sites. Such selective poisoning may be important in the control of bone growth.

## 2. Synthetic methods

### 2.1. Precipitation from solution

#### *2.1.1. Precipitation from a glassy polymer*

The precipitation of crystals from glassy polymers has been the subject of a number of studies in the context of fire retardants and stabilizers in polystyrene and the preparation of model composites. Work at Sussex on the precipitation of nitroanilines into polymers as part of a study of second-harmonic generation in composites [3] will be used to illustrate the principles. The solubility of a low molecular weight compound in a glassy polymer shows the same phase behaviour as the dissolution of compounds in liquids. Thus, as shown in Fig. 2, the solubility increases with temperature up to 100% at the melting point of the solute. The diagram would be more complicated in the event of liquid–liquid phase immiscibility.

In a solute–solvent system, the lower (solvent-rich) end of the diagram would normally be terminated by the crystallization of the solvent. For solutes in amorphous polymers, the diagram is effectively terminated by the glass transition temperature of the

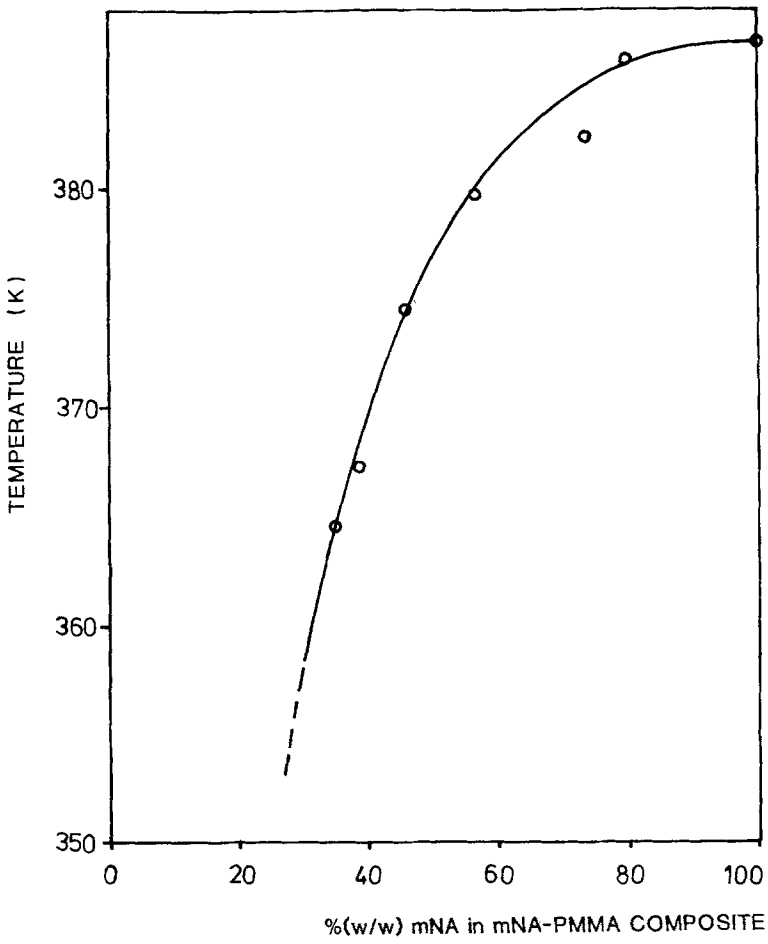


*Figure 2* Solubility curve for m-nitroaniline in poly(methylmethacrylate).

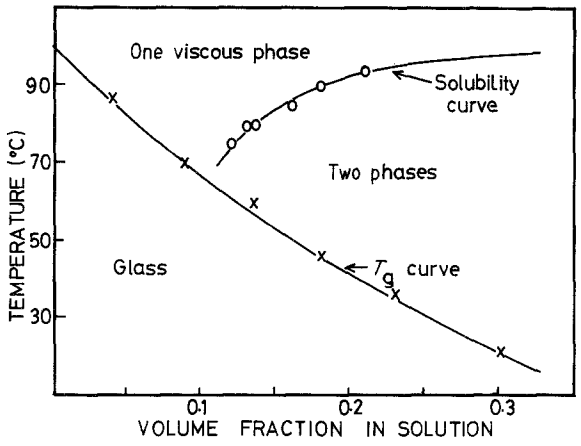


*Figure 3* Phase diagram for acetanilide and (styrene–acrylonitrile)-copolymer. After Joseph and co-workers [4].

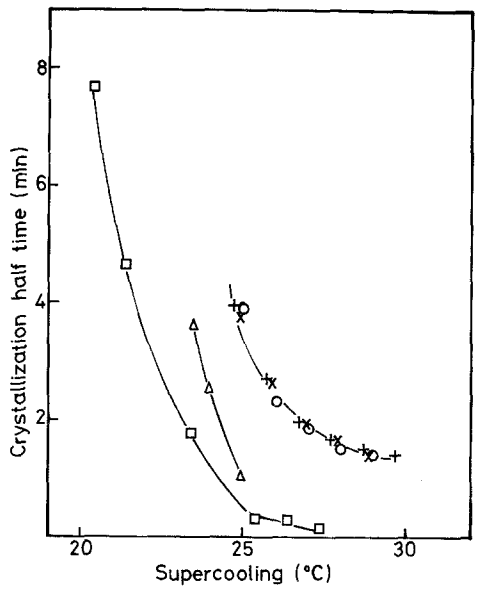


*Figure 4* Crystallization half-time for m-nitroaniline from polystyrene and from solvents, showing the retarding effect of polymers on crystal growth at equivalent supercoolings. (□) 37.5 wt % m-nitroaniline in toluene, (△) 31.3 wt % m-nitroaniline in benzene, (○) 18.4 wt % m-nitroaniline in polystyrene, (+) 14.2 wt % m-nitroaniline in polystyrene, (x) 13.9 wt % m-nitroaniline in polystyrene.

polymer, which is itself a function of the solute content. Fig. 3 also shows the downward trend of the glass transition with increasing solute content.

From the solute–polymer phase diagram, we can determine the conditions under which precipitation of crystals, within the polymer, should occur and the extent of precipitation at any composition and temperature. In order to follow the precipitation further, it is necessary to investigate the crystallization kinetics for the solute within the polymer. In the first instance, one would expect similar behaviour to crystallization from a concentrated solution, with the process slowed by the relatively high viscosity of the polymer. Fig. 4 shows the temperature dependence of crystalization half-time for precipitation of nitroaniline from polystyrene. When crystallization rate is expressed as a function of supercooling below the dissolution temperature, crystallization from solvents is faster under equivalent conditions, because of the higher viscosity of the polymer. Rapid cooling of polymer–solute mixtures takes the system through the glass transition and results in a glassy solution which can be crystallized on reheating (Fig. 5).

The morphology of the precipitate will be modified by virtue of its forming within the viscous polymer, rather than in a solvent. In the case of acetanilide growing with styrene–acrylonitrile copolymer the width of the needle-like crystals decreases with decreasing temperature of crystallization. For 2-methyl-4-nitroaniline (MNA) and metanitroaniline (mNA) growing from polystyrene the crystal size is much reduced, compared to crystallization from solvent, when solutions of similar composition are cooled at the same rate. The normal morphology of mNA crystals is long needles and from the polymer these form as spherulites with 1 to 10 $\mu$m fibres while MNA, which normally forms equiaxed crystals, forms as very fine (0.5 $\mu$m) particles from polystyrene.

Narkis and co-workers [6–9] have studied the precipitation from polystyrene of a number of halobenzenes, related to flame retardants. They observed that the softening temperature of the quenched polymer decreased by 15 to 30° C with increasing additive concentration, and then rose again at above 20% as the precipitated phase reinforced the polymer. On slow cooling, crystallization occurred about 15° C below the equilibrium solubility line observed on heating. The crystals formed as needles, dendrites or small crystals depending on the conditions. Oriented structures could be produced by shearing the sample during crystallization.

Kardos and co-workers [4, 5] produced samples of glassy styrene–acrylonitrile and of rubbery butadiene–acrylonitrile, reinforced with acetanilide or with anthracene, as models for the reinforcing effect of the crystalline phase in spherulitic polymers. Measurements of crystallization rate showed that this rose with supercooling, below the solubility line (liquidus) and then decreased again as the glass transition was approached. For a 17% acetanilide–polystyrene system the crystals formed as rods of 20 to 50 $\mu$m long and 5 to 20 $\mu$m diameter at 90° C. As the crystallization temperature was reduced to 45° C the diameter decreased to 0.1 $\mu$m.

Hannon and Wissbrun [10] studied the system calcium thiocyanate–"phenoxy" (the linear condensation product of bisphenol-A and epichlorohydrin) where the melt viscosity and the glass transition are increased by the additive.

### 2.1.2. Precipitation from a crystalline polymer

Many crystalline polymer–small molecule mixtures form eutectics, which is the simplest form of phase diagram for two compounds which are miscible in the liquid state, and do not form isomorphous crystals. Kitaigorodsky [11] has surveyed studies on phase diagrams of many small molecule–polymer systems. In general either eutectics were formed or there was no liquid–liquid miscibility. Smith and Pennings [12, 13] have studied eutectic formation in polyethylene–1, 2, 4, 5-tetrachlorobenzene [12] and in isotactic polypropylene–pentaerythrityl tetrabromide [13]. The phase diagram can be calculated using the Flory–Huggins theory of polymer solutions but Smith and

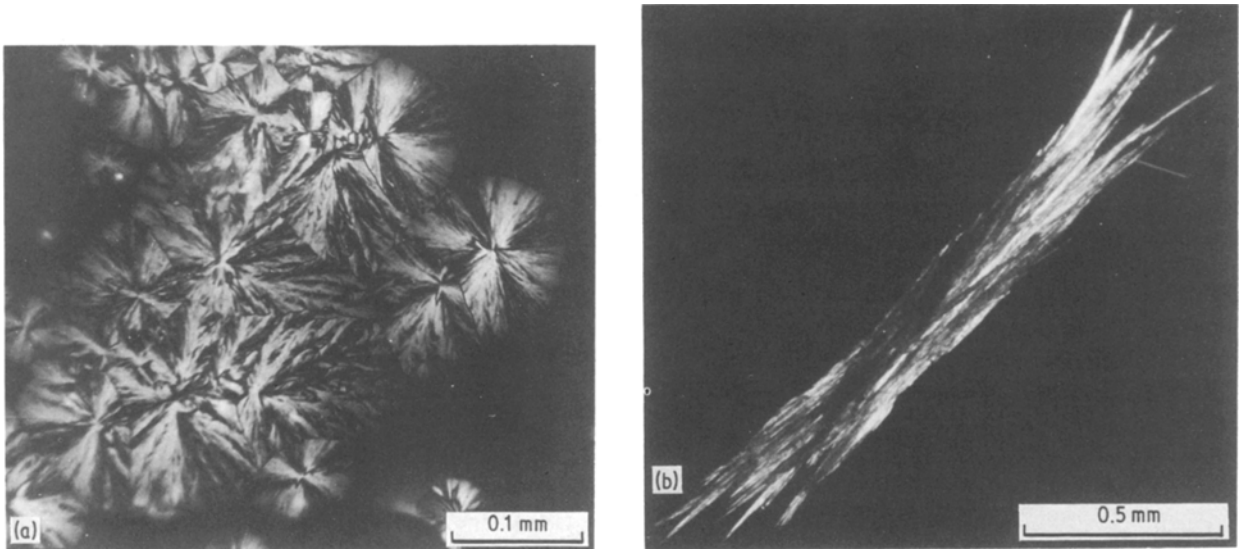


*Figure 5* 2-Methyl-4-nitroaniline crystals (a) growing from quenched polystyrene, (b) growing from ethanol solution. Both 7.5% solutions at room temperature.

Pennings found that the agreement with experiment was rather poor. This disagreement seems to originate largely in the 10° C difference between the observed melting point for polyethylene and the theoretical value used in the calculations [12]. Wittman and St John Manley [14] have studied blends of polycaprolactone with trioxane. They found good agreement between the form of the diagram and Flory–Huggins theory. Fig. 6 shows the phase diagram for benzoic acid in low-density polyethylene. The temperatures are melting peaks determined by differential scanning calorimetry of slowly-cooled samples. The left-hand liquidus represents the melting of polyethylene spherulites into a benzoic acid–polyethylene melt while the right-hand liquidus is melting of benzoic acid crystals into polyethylene. The eutectic then represents the temperature at which polyethylene and benzoic acid crystallize simultaneously from the same liquid. This picture, which applies to simple eutectics, is not strictly correct for polymers for two reasons: because the crystallization of polymers is slow and so occurs below the equilibrium melting temperature, and because polymers do not crystallize completely but always contain a certain amount of residual amorphous material. A full discussion of the effect of these factors on the observed phase behaviour has not been given.

In the case of a lower polymer melting point the eutectic point moves across toward the polymer axis, as shown for a polyethylene copolymer in Fig. 7. In theory, the eutectic point is that at which the melting temperatures of both crystalline phases in the melt are the same. Reducing the polymer melting point should thus move the eutectic down and toward the polymer axis. On the basis of a simple version of Flory–

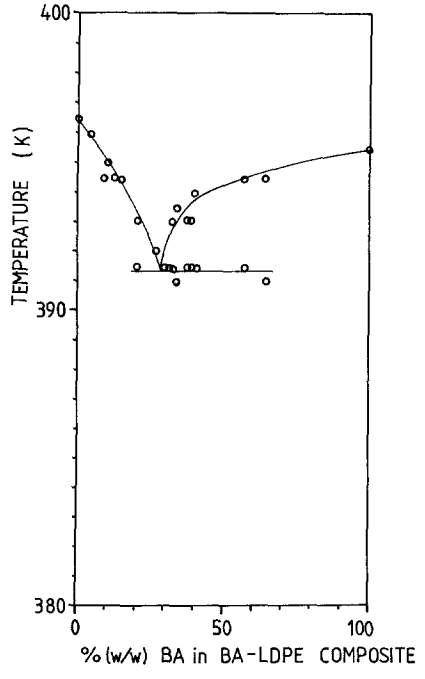


*Figure 6* Phase diagram for linear low-density polyethylene–benzoic acid, showing a eutectic point.

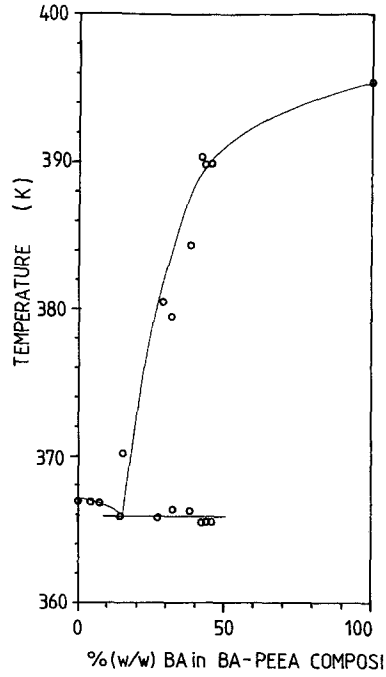


*Figure 7* Phase diagram for poly(ethylene-co-ethylacrylate) and benzoic acid. Compared to Fig. 6, the eutectic is moved towards the polymer axis due to the lower melting point of the polymer.

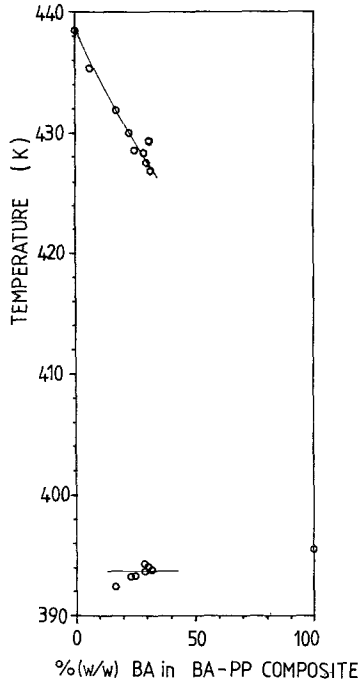


*Figure 8* Partial phase diagram for polypropylene–benzoic acid, showing immiscibility.

Huggins theory, Smith and Pennings [12] argue that the melting point of the polymer and additive must be quite similar if a eutectic point is to be observed rather than being very close to one axis or the other. The studies of Rosso, and co-workers [15–17] on eutectics between polyesters and various solvents show that this is partly true but there are many systems which show melting point differences of 50° C yet still give clear eutectics. Reducing the crystallinity but not the melting point, by block copolymerization or by adding a high-molecular weight atactic polymer, for instance, has no effect on the position of the eutectic.

When liquid immiscibility occurs as in polypropylene–benzoic acid, the melting of the two components are essentially unaffected (Fig. 8).

Myasnikova *et al.* [18] have found one system, polyethyleneoxide–resorcinol, in which a molecular complex is formed at a mole ratio of 2 : 1 monomer units : resorcinol.

A number of factors will modify the crystallization kinetics of the eutectics when compared to the pure polymer. At constant supercooling, the low molecular weight additive lowers the viscosity and so can increase the growth rate, particularly if the glass transition temperature of the polymer is approached. In the system polyethylene–tetrachlorobenzene, Smith and Pennings [12] found that the supercooling at which crystallization occurred increased from about 1° C to 10° C on approaching the eutectic composition from pure tetrachlorobenzene. In addition, either phase may enhance nucleation of crystals of the other. Polypropylene is nucleated by pentaerithrityl tetrabromide crystals [13].

According to the theory of Jackson and Hunt [14, 20] for metal rod eutectics the size of the rods is governed by the interfacial energy between the two solid phases. Smith and Pennings had some success in using this theory for pentaerythrityl tetrabromide–polypropylene. We could also apply with similar success the theory of Keith and Padden [21, 22] for spherulitic crystallization in which the morphology of the solid eutectic will be determined by the characteristic diffusion distance for the components during the crystallization process; this is of the order of $D/G$, the ratio of diffusion rate $D$ to growth rate $G$. At slower growth rates, in a temperature gradient, the structure consisted of polypropylene spherulites and large additive crystals.

When, on cooling, the polymer crystallizes first, the low molecular weight material may be entrained in the growing spherulite or may segregate into the liquid phase ahead of the growth front. In studies of the behaviour of small concentrations of additives in polypropylene, Ryan and Calvert [23] showed that the degree of segregation ahead of a growing spherulite depended on the rate of advance of the growth front in relation to the diffusion rate of the low molecular weight additive. When the solute crystallizes first, it forms larger crystals with the fine-scale eutectic then filling in between them. Thus, crystallization on the solute-rich side of the eutectic would be expected to give a relatively coarse morphology which is largely characteristic of the impure solute. On the polymer-rich side of the eutectic, the polymer should first form as spherulites, leaving the solute very finely divided in the interlamellar regions.

A study of the effect of pressure on the polyethylene–1, 2, 4, 5-tetrachlorobenzene phase diagram [24] showed that the normal high-pressure disordered phase of polyethylene did not form and that the formation of extended chain crystals was suppressed.

Aromatic halides are used as fire-retardants, and Chang [25] has described the effect of a number of commercial additives on polypropylene. Those additives which are solid at the crystallization temperature of the polymer act as nucleating agents while the soluble additives increase the spherulite growth rate and give rise to large spherulites.

There are a number of systems where inorganic salts are soluble in polar polymers. There have been extensive studies of the dielectric properties of polyethylene oxide–salt complexes [26, 27] and these are of importance as battery electrolytes [28]. Lithium halides are soluble in nylons and their effect on the melting and crystallization behaviour have been studied [29].

The attraction of the polymer-additive eutectics is that they could allow formation of a finely dispersed and highly oriented crystalline phase reinforcing the polymer. A second approach to a similar structure is to swell the polymer with an additive solution and then induce precipitation by allowing the solvent to evaporate. Moskvina *et al.* [30] have produced such composites of oriented tridecanoic acid crystals in drawn polyethylene and polytetrafluoroethylene films.

### 2.1.3. Properties and morphology

The mechanical properties of polymer–crystal composites have been studied by Kardos and co-workers [4, 5]. For the toughness associated with the polymer it is desirable to have the organic solute embedded in the polymer rather than vice versa. It would be expected

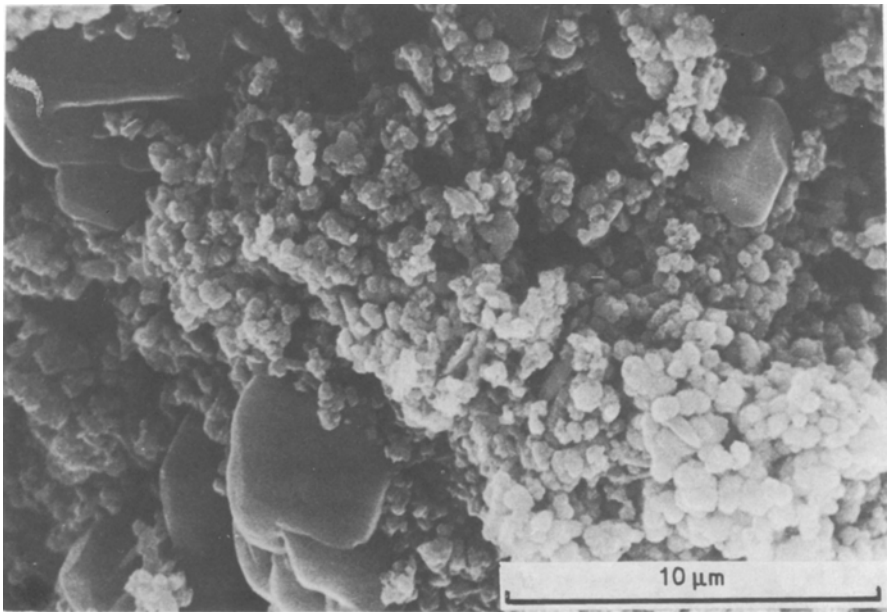


*Figure 9* Particles of iron oxide precipitated from iron acetylacetonate dissolved in poly(methylmethacrylate). The polymer has been washed away by dichloromethane to reveal the particles.

that this would be the case up to high levels of solute as long as the solute crystallizes before the polymer. In the event of a small amount of polymer separating out first, we would then have a continuous solute phase which would be expected to form a brittle composite. Naturally the toughness and extensibility of the composite will decrease as the polymer content decreases from about 50 vol %.

Conducting polymer composites have been prepared by precipitating organic metals from polymers. Thus the conducting salt TCNQ–TTT was cast from solution with polycarbonate in dichlorobenzene [31–33]. The salt formed as whiskers and fibrous dendrites which rendered the composite electrically conducting at 1 wt % salt, much below the 20 to 30% that would be expected for spherical particles in a matrix. Similar structures form when thiapyrylium dyes form crystals of a complex with polycarbonate which shows greatly enhanced photoconductivity compared to the pure dye [34, 35].

## 2.2. Precipitation by reaction

The growth of composite structures by precipitation of a species from solution in a polymer is limited by the need for the precipitate and the polymer to be miscible at high temperatures or in a common solvent. A much wider range of composites can be prepared if the precipitate is chemically formed within the polymer from a soluble species. A variety of composites of polymers with metals or metal oxides have been produced in this way.

In our laboratory we have been studying the preparation of composites of iron and iron oxides in polymers by direct precipitation. An amorphous hydrated iron oxide has been formed in several polymers by incorporation of either iron(III) chloride or iron(III) acetylacetonate into solution with the polymer, then casting a film which is subsequently treated with aqueous base. Particles are of the order of 1 $\mu$m (Fig. 9). Subsequent treatment of the film with iron(II) sulphate solution lead to the formation of magnetite. Iron metal can be formed by the treatment of films containing iron chloride with aqueous sodium borohydride, the metal being formed predominantly as a surface film. Similar treatment of a film with sodium naphthalide in tetrahydrofuran gave fine particulate iron within the film. Clearly the site of reaction and the morphology of the precipitate is partly determined by the relative mobilities of the reacting species [36].

Mark and co-workers [37–41] have blended silicone rubbers with liquid silicon tetraethoxide. The alkoxide was allowed to hydrolyse within the solid rubber by exposure to moist air such that it converted to finely divided silica which simultaneously acts as a filler and a crosslinker [37]. Electron microscopy shows particles of 10 to 20 nm [38]. Up to 17 wt % filler has been incorporated [39]. Up to 65 wt % (30 vol %) titania has also been incorporated into PDMS by *in situ* hydrolysis of titanium tetra-n-propoxide [40, 41] although this volume fraction of particles is rather higher than would be expected, based on the starting composition (70 wt % titanium tetrapropoxide) if the particles were fully dense titania.

A number of groups have explored the production of particles of magnetic metals in polymers by decomposition of metal carbonyls. Hess and Parker [42] prepared cobalt particles of 10 to 100 nm by thermal decomposition of dicobalt octacarbonyl in solutions of various polymers. The polymer promoted formation of single domain particles rather than large multidomain particles. In some cases the particles formed chains which had high coercive forces and remanence ratios. Decomposition of cobalt carbonyl in solid polystyrene produces particles of 10 to 30 nm [43]. Smith and Wychick [44] made similar dispersions of up to 8% of 10 nm iron particles by thermolysis of iron pentacarbonyl in polymer solutions. Suitably functional polymers were shown to catalyse the decomposition and particle nucleation. This approach has been extended to precipitation into solid polymers by Reich and Goldberg [45] who prepared iron and magnetic $\gamma$-$Fe_2O_3$ in a variety of polymers by carbonyl decomposition. Up to 20 wt % iron oxide was

incorporated into polyvinylidene fluoride. In very thin films the oxide formed 10 nm particles while in bulk samples 0.5 $\mu$m clusters were seen. Iron oxide has been incorporated into polytetrafluorethylene at up to 5 wt % by treatment with iron carbonyl followed by oxidation in air [46]. The particle size was about 4 nm. A similar treatment of polyethylene and polypropylene with iron pentacarbonyl followed by aqueous potassium permanganate gave adherent surface films of iron and manganese oxides [47].

Magnetite and silver oxide have been formed by base treatment of phospholipid vesicles containing a metal salt [48, 49] and this process could be extended to composites.

Kovacs and Vincett [50–52] have published a number of papers on the evaporation of metals, especially selenium, or salts on to soft polymer surfaces. Inorganic films tend to form subsurface particles while organic materials remain partly embedded at the surface. This effect is determined by the various surface tensions. What is more surprising is that the inorganic particles form as a monolayer of uniformly sized particles a few nanometres below the surface. As evaporation proceeds the spherical particles increase in diameter but maintain a constant area coverage and do not form continuous films until, at about 0.4 $\mu$m, particle coalescence becomes too slow to balance the influx of metal. Tin particles have been incorporated into polymer films by sputtering during film formation by plasma polymerization [53].

A method has been described for the production of polymer–metal composite coatings by dispersion of zinc oxide or other metal oxides into polymers followed by electrochemical reduction [54]. As the reduction occurs the coating becomes highly conducting with a continuous network of metal particles. A related process for conducting composites is to coat polymer beads with metal by electroless deposition, then compression-mould the beads so as to preserve the metal continuity [55].

There have been a number of reports of conducting composites made by the decomposition of metal salts in polymers. Polyimides have been doped with silver, gold or palladium salts which decompose to metal during curing of the resin at 200 to 300° C. The surface resistivity of polyimides has also been modified by the inclusion of cobalt salts which precipitate as oxide beneath the surface [56]. In some cases the metal forms as a surface mirror which makes the film highly conducting at low metal contents [57–60]. Silver has also been formed in fine conducting lines in polyimide by laser decomposition of dissolved silver nitrate [61]. Copper sulphide and cadmium sulphide dispersions in polymers have been prepared and become highly conducting at 40 wt % sulphide, and electrically conducting copper sulphide-treated polyacrylonitrile fibre is reported to be commercially available [62]. A number of recent papers from the DuPont company have described the formation of layers of silver chloride and of silver within polymer films by countercurrent diffusion of reagents from the film surfaces [63, 64].

Reduction of metal salts in solution has been used to prepare colloidal suspensions. Recently the preparation of amorphous iron–cobalt particles by reduction of metal salts with $KBH_4$ in aqueous solution has been reported [65]. Copper salts have been similarly reduced in polymer solutions where the polymer acts to stabilize the dispersion and modify the catalytic activity of the particles [66, 67]. Copper has been precipitated into cellulose to 18 wt % by first dissolving the cellulose into a basic copper solution and then reducing it [68].

## 3. Related *in situ* precipitation

### 3.1. Glass–ceramics

There are a number of cases where precipitation processes, similar to those discussed here, are used to produce composite materials. A typical glass–ceramic system is lithia–silica–alumina where a fine-grained precipitate of $\beta$-spodumene or $\beta$-quartz is formed by reheating the glass to a crystallization temperature of around 1090° C [69]. A nucleating addition of titania, or a metal such as gold, is frequently used. The titania phase separates and then crystallizes as $Al_2Ti_2O_7$ during a lower-temperature (900° C) nucleation treatment. The nucleation treatment is carried out just above the glass transition temperature, to obtain abundant nuclei. The resultant glass–ceramic is from 50 to 100 vol % crystalline with a very fine crystal size, around 1 $\mu$m. A key concept in the development of these systems is the relative shift of the nucleation and growth curves as seen in Fig. 10, such that either a two-stage heat treatment must be used, or the treatment temperature must be carefully chosen to allow both processes to continue. By extrusion of the crystallizing melt it is possible to orient the crystals [69]. At very high nucleation levels it is also possible to form transparent composites containing particles of less than 100 nm [69].

Glass–ceramics can also be oriented by crystallization in a temperature gradient. This method has also been applied to a number of eutectics including glass-forming oxides and salts [70]. Highly aligned lamellar or fibrous structures were produced, on a scale that decreased from 10 $\mu$m to 1 $\mu$m as the crystallization

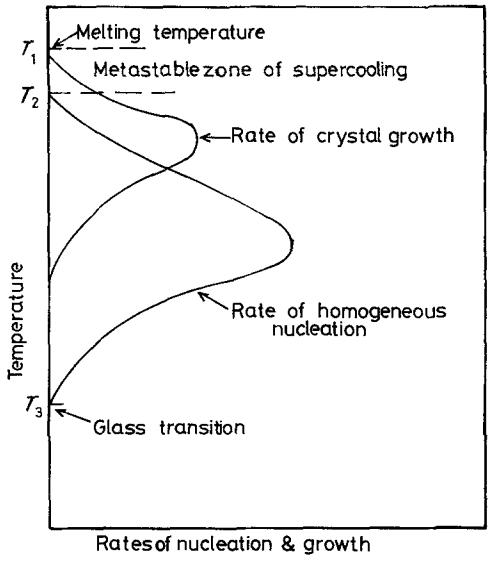


*Figure 10* Schematic nucleation and growth curves for a glass-forming system.

rate increased. Similar structures have been formed in metal alloys and are also termed "*in situ*" composites [71]. In a similar vein, Kiss [72] has recently described composites of liquid crystalline polyesters and glassy polymers. During extrusion the liquid-crystalline polymer forms fibres within the glassy matrix. The two polymers are probably immiscible in the liquid state.

### 3.2. Gels

Gels have been used as supports for crystal growth for some time [73]. Gels of all types have been used including synthetic polymers, silica gels and biological polymers. For the growth of single crystals, the gel allows concentrations to be varied by diffusion of the precipitants into the gel such that a range of conditions may be tested at once. The gel suppresses precipitate growth by aggregation, which may often be the dominant process for very insoluble species, and prevents secondary nucleation due to collision and fragmentation processes. Thus a recent paper on iron oxide precipitation in gels argues that they can give a clearer view of the true morphology of colloidal precipitates [74].

## 4. Biological composites

### 4.1. Mechanisms of formation

In the previous sections we have reviewed the major approaches adopted in the formation of synthetic composite materials by direct precipitation. Although these methods have resulted in considerable success in the design of new materials they remain relatively unsophisticated when compared with biological composites such as bone, teeth and shells. The variety and complexity of biominerals reflects a diversity of chemical and biological processes such that any attempt to classify these mechanisms will have exceptions. However, some rationalizations can be made which illustrate the general strategies of composite formation, and, in particular, highlight the role of macromolecules in the mediation of mineral deposition.

Biominerals are formed by the initial extracellular deposition of a polymer matrix which is subsequently infilled with mineral. Growth of the composites in extracellular environments requires that the cells control both polymer and mineral deposition over relatively large distances (often micrometres away) and this is achieved locally through the regulation of mass, charge and energy transfer via concentration, electrochemical, proton (pH) and redox gradients in the extracellular space. The kinetic control of ion flow between the cells and the polymeric matrix is a fundamental aspect in the biological mediation of composite formation since the level of supersaturation, solution pH and composition (ionic strength), and concentration of inhibitors and promotors are all optimized.

At low concentrations polymers in solution are habit modifiers for crystal growth, for example sodium chloride crystals are affected by low concentrations of polysaccharides [75], by selective adsorption to and poisoning of specific growth faces. The growth habit will generally be affected by the polarity and adsorption properties of the growth medium but no specific effects have been reported in concentrated polymer systems. These processes are believed to be important in the biological mineralization of bones and shells. For instance it has been reported that proteins rich in aspartic acid, found in mollusc shells, affect the habit of calcite crystals [76, 77]. Another example of a highly specific interaction is the effect of "antifreeze" glycopeptides present in the blood of polar fish. At 0.5% of the polymer, the freezing point of water is reduced by 0.5% and the habit of the ice crystals is changed [78]. The melting point is effectively unchanged. These specific effects of adsorbed polymers on growing precipitates would be of major importance in any effort to build up complex structures, analogous to biological composites, by *in situ* precipitation.

A key concept in the formation of organized biological composites such as enamel (Fig. 1) is that the chemical, structural and topographical nature of the matrix surface is such that molecular interactions at the mineral–matrix interface result in the regulation of the mineral phase. Nucleation of the mineral particles occurs at specific sites on the matrix macromolecules and the direction and extent of crystal growth is well defined. The influence of the matrix macromolecules at the mineral surface will be dependent on the correspondence between the charge density, topography (kinks, steps, surface roughening), lattice geometry (epitaxis) and stereochemistry of the crystal faces, and of the polymer. Crystal/particle size, polymorph selectivity, morphological selectivity and crystal orientation are all mediated by the macromolecular framework.

In conclusion, there are three key features which biology adopts in the controlled deposition of mineral particles within polymeric matrices: (i) ion-flux regulation at the matrix interface, (ii) growth and habit modification by soluble molecules present within the matrix, and (iii) crystallochemical mediation of nucleation and growth by molecular-specific interactions at the polymer surface.

### 4.2. Classification and characterization of biocomposites

The interplay between the different molecular interactions which may occur at a mineral–matrix interface during biomineralization can generate different types of composite according to the combination of matrix-mediated processes exhibited by the system. The extent of matrix intervention present spans a wide continuum in different systems so there is bound to be overlap and complication in attempting a classification. However, the end-members of these series can be clearly identified. The following classifications can be established (Table I).

#### *4.2.1. Type I (matrix-inert) biocomposites*

Matrix-inert (Type I) biocomposites arise from passive molecular interactions at the matrix–mineral interface which result in non-specific nucleation and spatially restricted growth. Mineralization is not crystallographically oriented and the polymorph structure and morphology (geometric or irregular) is determined by the physicochemical properties (under biological control) of the mineralization zone. The particle

TABLE I Classification and characterization of biocomposites: matrix-mediated processes

| Type | Crystal nucleation | Growth | Particle size* | Particle morphology* | Crystallographic orientation* | Polymorph adoption* | Matrix function | Examples |
|---|---|---|---|---|---|---|---|---|
| I (matrix-inert) | Non-specific | Spatially restricted | x | x | x | x | Heterogeneous nucleation catalyst, mechanical support | Chiton teeth, algae, granular foraminifera |
| II (nucleation) | Site-directed, regiospecific | Spatially restricted | x | x | √ | √‡ | Crystal nucleation control, mechanical support | Avian egg shells, radial foraminifera, limpet teeth (cusps) |
| III (amorphous) | Inhibited† | Regulated (vectorial) | √ | √§ | x | √ | Growth control, polymorph stabilization, mechanical support | Plant silica diatoms, cystoliths invertebrate granules |
| IV (oriented) | site-directed regiospecific | Regulated (vectorial/periodic) | √ | √ | √ | √ | Crystal nucleation and growth control, mechanical support | Mollusc shells, bone, enamel |

*√ Controlled by matrix; x uncontrolled.
†Matrix has no nucleation influence on biogenic silica. The amorphous nature of this mineral is governed by physicochemical factors.
‡Physicochemical mediation may also be involved.
§Mediation of microscopic (not crystallographic) morphology.

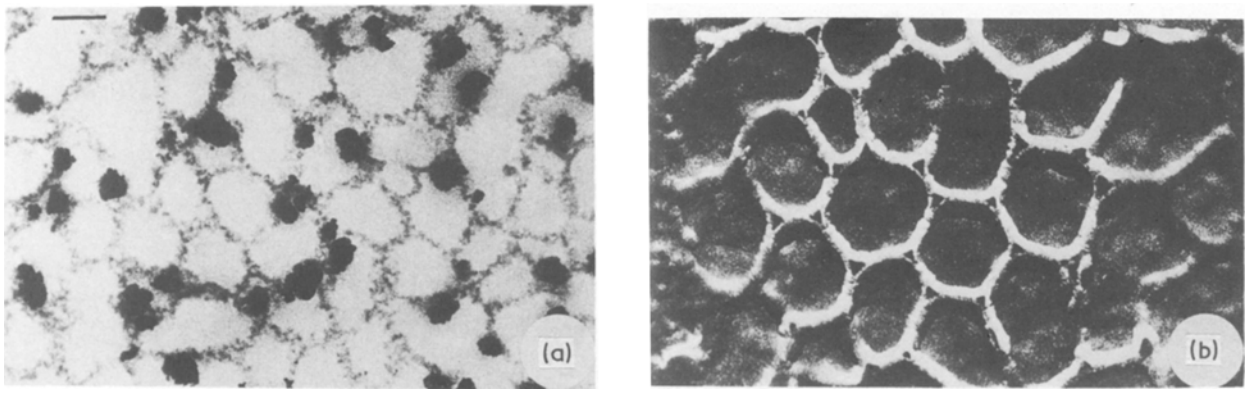


*Figure 11* Magnetite mineralization in chiton teeth. (a) Initial stages of mineralization showing magnetite crystals deposited on a fibrous organic framework; (b) late stage in mineralization showing the polygonal framework totally impregnated with magnetite. Scale bar = 100 nm in both photographs. Reproduced with permission from Towe and Lowenstam [79].

size distribution is heterogeneous and large crystals may grow at the expense of small ones (Ostwald ripening). The function of the matrix lies in mechanical support and (possibly) in non-specific nucleation catalysis.

An example of a Type I biocomposite can be found in the radular teeth of chitons [79]. The molluscs secrete an extracellular three-dimensional polysaccharide matrix of fibrous chitin-like material which acts as a spatial frame for subsequent deposition of the mineral magnetic ($Fe_3O_4$). Precipitation begins at the edges of the polymer matrix and gradually proceeds to fill in the interspaces in the organic net, such that there is a random crystallographic orientation (Fig. 11). The matrix therefore acts as a non-specific surface for nucleation and growth and provides a spatial (volume) constraint on the development of mineralization. Its primary function lies in the mechanical design of the teeth in relation to the specialized cutting (rasping) action required to remove algae from the rock surface.

### 4.2.2. Type II (*nucleation*) biocomposites

These biocomposites combine the matrix-mediated processes of site-directed and spatially organized nucleation. Since nucleation is primarily dependent on surface free energy (at constant supersaturation), the chemical, structural and topographic nature of the loci is such as to minimize interfacial energy as a function of crystal structure and orientation. Type II biocomposites show minimal evidence of active matrix mediation of crystal growth. Characteristic features include discrete nucleation sites organized periodically across the polymeric matrix (regiospecificity) and crystallographic orientation of the nuclei. These properties direct crystal growth along a preferred crystal axis although no active modulation of growth occurs after nucleation. Therefore, although there is orientation of the crystals, the absence of matrix intervention in crystal growth results in a heterogeneous particle size distribution and morphologies which are irregular or characteristic of inorganic precipitates. The function of the matrix lies in nucleation control which dictates the structure, spatial organization and orientation of the initial mineral deposits as well as acting as a fibrous network for structural support.

An example of a Type II biocomposite is the avian eggshell. The inner surface of the shell comprises a mesh of fibrous disulphide-linked proteins (the shell membranes) intimately associated with polysaccharide material. The boundary of the membranes with the shell contains regiospecific loci of spherulitic protein masses (cores) which provide the active sites for calcite nucleation (Fig. 12).

Although no details are known concerning the molecular interactions at the protein core–calcite interface, the specificity of these centres is reflected in the preferential radial development of crystals along the [0 0 1] direction. Outgrowth from the cores continues without active matrix intervention and becomes spatially restricted by the presence of crystalline material from adjacent cones, by polymer secreted

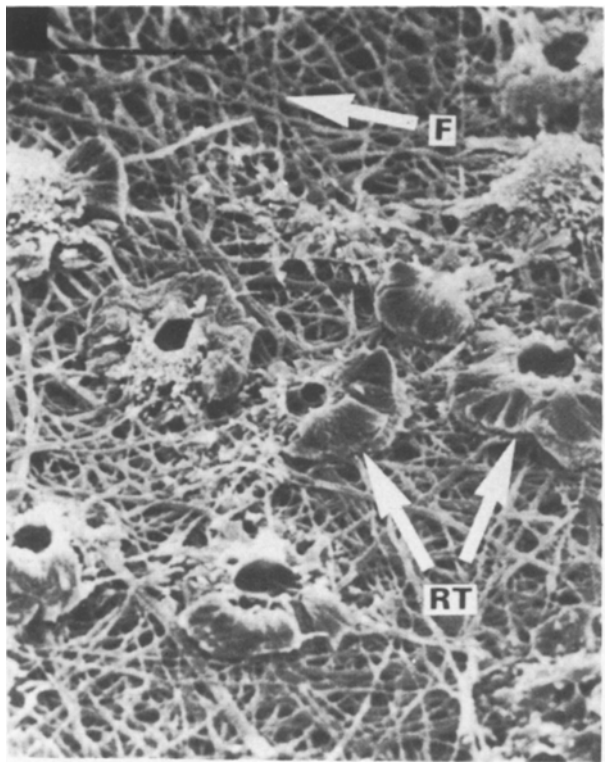


*Figure 12* Scanning electron micrograph showing the fibrous shell membrane (F) from the inner surface of the eggshell of the Great Crested Grebe. The ruptured tips (RT) of the cones indicate the regiospecific sites of calcite nucleation. Scale bar = 50 μm. Reproduced with permission from Board *et al.* [80].

into the shell palisade layer, and by the underlying shell membranes. In addition, changes in the nature of the matrix (structure, composition and rate of secretion) within the palisade layer results in a gradual randomization of the initial *c* axis orientation by growth hindrance and subsequent secondary (non-oriented) nucleation on existing crystal surfaces [81].

### 4.2.3. Type III (amorphous) biocomposites

Biocomposites comprising amorphous mineral phases can arise from active matrix-mediation in both nucleation and vectorial growth processes. In some materials, for example those containing amorphous calcium carbonates and phosphates, the matrix acts as a specific inhibitor of crystal nucleation; in other biominerals such as silica, non-crystallinity is determined by physicochemical properties [2]. The control of both direction and extent of growth is determined by the microarchitecture of the polymer framework and, since amorphous materials have no intrinsic crystallographic habit, they can be moulded into a myriad of shapes. This infinitely adaptive morphology is highlighted in the complex structures of the silica shells of diatoms [82]. The major functions of Type III biocomposite matrices include the selective stabilization of amorphous phases, particle growth control and mechanical support.

An example of a Type III biocomposite is the amorphous calcium carbonate deposits (cystoliths) formed in the leaves of many higher plants. Ultrastructural and chemical studies have revealed the selective stabilization and organization of these non-crystalline deposits by polymer substrates. The biological control of cystolith formation is reflected in the bulk morphology which is species-specific, often with elaborate surface structures (Fig. 13a). Demineralization of the cystoliths with ethylenediaminetetraacetic acid (EDTA) indicates that the particles are encased in an organic sheath under which is a net of polysaccharide intimately associated with the growth of the mineral phase (Fig. 13b) [83].

In plant silica, the deposition of Type III biocomposites is associated with precise morphological order at the microscopic level [84]. A range of structural motifs such as sheet-like, fibrillar and globular substructures is generated from the ordered aggregation of preformed amorphous particles. The motifs are formed at different stages of mineralization and can be linked to compositional changes in the nature of the polysaccharide matrix deposited at the sites of mineralization. Presumably, the spatially organised decoration of the underlying polysaccharide matrix reflects the stereochemical nature, i.e. the arrangement of charged residues and hydrogen-bonding centres, of the matrix surface.

### 4.2.4. Type IV (oriented) biocomposites

Type IV biocomposites are the most complex and highly organized biominerals known. They combine the processes of site-directed and regiospecific nucleation with vectorial growth regulation. In addition, the processes are coordinated spatially and temporally such that oriented composites are constructed.

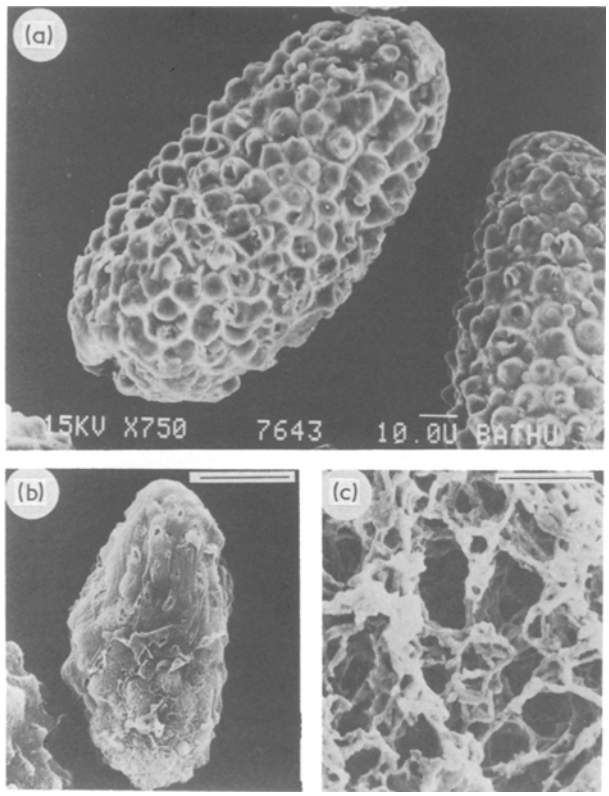


*Figure 13* Scanning electron micrographs of cistoliths isolated from the leaves of *Fiscus retusa*; (a) untreated, scale bar = 10 μm; (b) decalcified showing organic sheath and internal polymetric matrix, scale bar = 25 μm; (c) high magnification image of the fibrous internal matrix from a decalcified cystolith, scale bar = 500 nm. Photos (b) and (c) courtesy of Dr M. Okazaki, Department of Biology, Tokyo Gakugei University.

Characteristic crystallochemical properties which are matrix-mediated include crystal size, morphology, crystallographic structure and growth orientation. The function of the matrix lies in nucleation and growth regulation and mechanical support.

Type IV biocomposites have been extensively studied both structurally and compositionally. For example, the nacreous inner surface of many mollusc shells is constructed from alternating layers of aragonite and organic matrix aligned parallel to each other such that each thin (30 to 300 nm) sheet of matrix is sandwiched between polygonal blocks of mineral (Fig. 14). Each individual matrix layer comprises an insoluble core of silk-fibroin-like proteins covered on both sides by layers of EDTA-soluble matrix constituents. In some species there is a thin β-chitin layer sandwiched between two layers of the insoluble protein matrix (Fig. 15). The relative concentrations of these constituents vary between shells of different species [87] and between different shell layers of the same species [88]. However, these comparative studies have shown that the EDTA-soluble extract is remarkably similar in all species studied to date and comprises a heterogeneous mixture of two classes of proteins [89]; (i) proteins rich in aspartic acid and, to a lesser extent, glutamic acid possibly with some covalently-bound sulphated polysaccharides, and (ii) proteins rich in serine associated with relatively large amounts of sulphated polysaccharide. In contrast, the EDTA-insoluble fraction varies considerably in composition

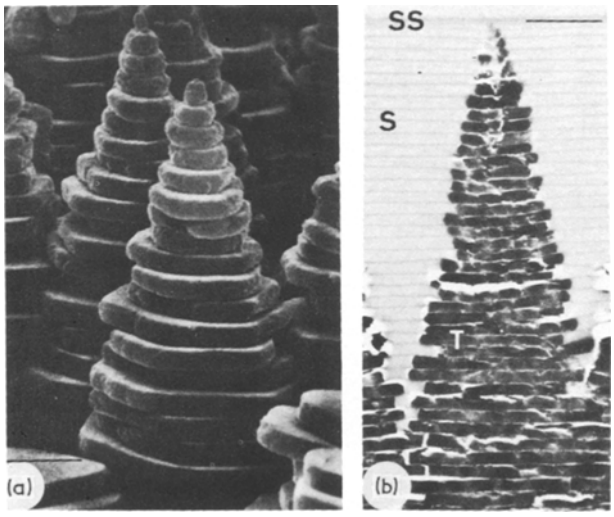


*Figure 14* (a) Growth surface of the nacreous layer from the mollusc *Monodonta labio* showing a stacked arrangement of the aragonite crystals. Scale bar = 2.5 $\mu$m. (b) Unstained section showing growing stack (T) with organic sheets (S) periodically interspersed between the aragonite crystals; (SS) = surface sheets. Scale bar = 4 $\mu$m. Reproduced with permission from Nakahara [85].

between different species. The major components are proteins rich in glycine, alanine, phenylalanine and tyrosine [90].

X-ray and electron diffraction [86, 91] indicate that the predominant configuration adopted by the insoluble proteins is the antiparallel $\beta$-pleated sheet and that the mean chitin fibre direction is perpendicular to the protein polypeptide chains, resulting in a plywood-like construction. It is assumed that the soluble matrix components are aligned with the antiparallel $\beta$-pleated sheet polypeptide chains of the core macromolecules such that they provide a charged interface between the rigid insoluble framework and the depositing mineral.

This simple two-component model of the molluscan organic matrix provides both the inherent rigidity and interfacial activity required. The stereochemical periodicity of the insoluble framework and interfacial macromolecules suggests a possible epitaxial role for the matrix, and this has been confirmed by electron diffraction of small (6 $\mu m^2$) regions of partially demineralized nacreous layer fragments, cooled to $-100°$ C to reduce electron irradiation damage. The results indicate a well-defined spatial arrangement between the matrix and aragonite crystallographic orientations within localized regions of the shell, with both the *a* and *b* axes of the antiparallel $\beta$-pleated sheet and the aragonite lattice matched in orientation at the interface (Fig. 16) [91]. The presence of negatively charged aspartic acid residues linked to the $\beta$-sheet configuration could act as a structured nucleation site for calcium binding in a configuration corresponding to the *ab* plane of aragonite. Comparison of the Ca–Ca distances in the *ab* plane of aragonite with the matrix periodicity indicates that a close matching occurs along the *a* axes (496 and 475 pm, respectively) whereas a greater mismatch is observed along the *b* axes (797 and 690 pm, respectively). However, the periodicities along the *b* axes are essentially commensurate over a distance of seven calcium atoms (480 pm) Fig. 17).

Since calcium binding to carboxylate groups is generally cooperative involving at least two or three ligands, an amino-acid sequence of Asp–X–Asp (where X is a neutral residue) along the $\beta$-sheet framework has been suggested to be the optimum binding and hence nucleation configuration for calcium at the matrix interface [93]. Domains along the $\beta$-sheet which do not conform to this sequence would then be inactive as nucleation sites. Thus the coding of such sequences at intervals along the $\beta$-sheet framework could provide the regiospecificity required to control the crystal dimensions in the *ab* plane, and the subsequent shell architecture. This implies direct genetic control of nucleation via protein replication.

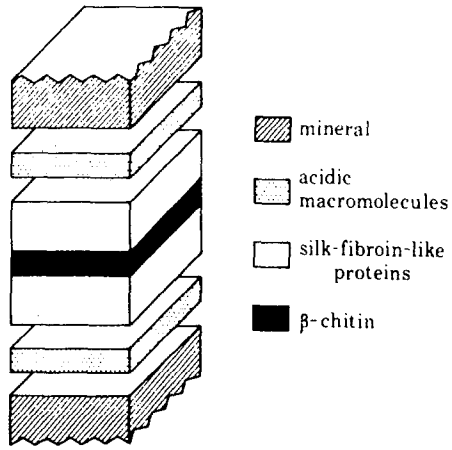


*Figure 15* Schematic representation of a composite section of a mollusc shell showing one individual matrix sheet bounded by mineral (aragonite). From Weiner and Traub [86].

The extent of crystal growth, i.e. crystal size, of the aragonite polygons in mollusc shells can be determined by the interaction of matrix surfaces which results in complete molecular inhibition of the growth sites. The complete blocking of growth sites in this way provides a means of directing the spatial organization of the biocomposite. For example, the "stacked" nacreous layer configuration shown in Fig. 14 is characterized by aragonite pseudohexagonal tablets which are restricted in thickness along the *c* axis due to interlamellar matrix sheets. Thus the temporal pulsing of matrix secretion determines the extent of crystal growth along the *c* axis and results in crystals of relatively uniform thickness. In addition, the formation of the alternative "brick wall" shells can be rationalized on a similar model except that the episodic deposition of the matrix layers occurs after the crystals in each layer have come into contact, whereas in the "stacked" model the matrix is secreted prior to horizontal contact of the crystals. An interesting corollary of this rationalization is that each interlamellar matrix layer has dual functionality, serving both as an inhibitor of crystal growth and as a nucleation surface for aragonite deposition.

## 5. General possibilities

As has been pointed out above, most biological composite materials are produced by an *in situ* precipitation process. Apart from special examples such as glass–ceramics, there are no commercial synthetic materials made in this way. The major aim of this review is to illustrate the possibilities.

There are a number of commercial or developmental

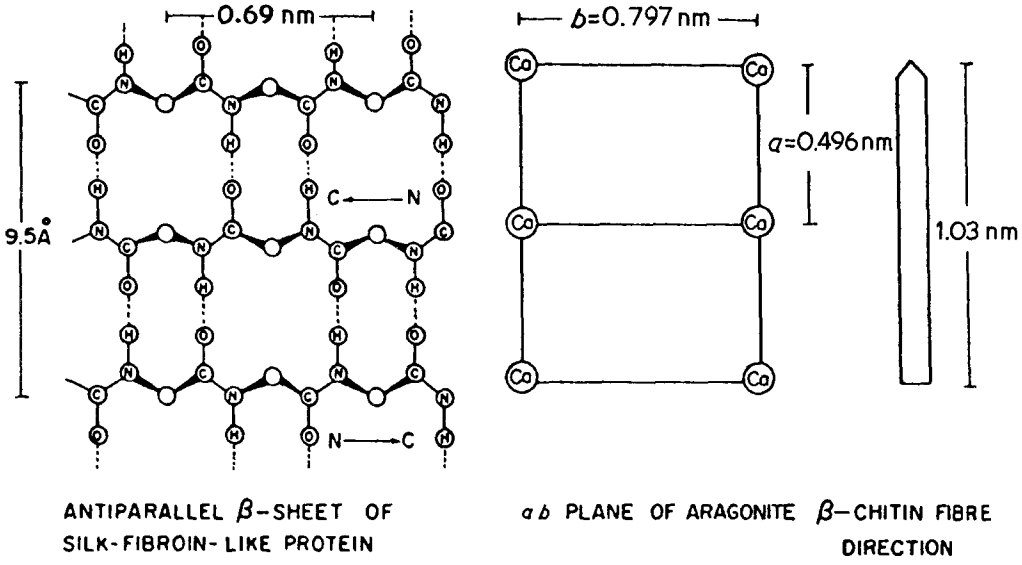


*Figure 16* Schematic representation of the structural relationships between protein sheets, aragonite crystals and chitin fibres in the nacreous layer of *N. repertus*. After Weiner and Traub [86].

composites which would apparently lend themselves to this approach. These include magnetic coatings made by the dispersion of iron oxides into resins and piezoelectric composites [94]. In terms of the application of these materials, a number of questions need to be answered to define their potential. These include: (i) what kinds of particles may be precipitated? (ii) How long does the process take? (iii) What levels of particle content can be reached? (iv) How much control can be exerted over the deposition?

We have discussed above a variety of routes for the formation of precipitates within a solid polymer, including precipitation from solution and chemical treatments. The only real restriction is that the process be compatible with the polymer, which limits the temperature range to below about 250° C and prevents the use of strong oxidizing agents. Many oxides, sulphides and metals as well as organic crystal have so far been produced by suitable routes. Many of these low-temperature precipitations do lead to amorphous particles of such strongly bonded materials as the oxides. The ability to produce crystalline precipitates will depend on the initial chemistry of the precipitation and on the conversion temperature during a subsequent heat treatment. Amorphous, hydrated iron oxide is known to convert through a series of forms to haematite over the temperature range from 200° C [95].

Precipitation from solution in a polymer can occur on a time-scale similar to that of polymer crystallization, which is usually rapid. The time taken for a chemical precipitation reaction depends on the thickness of the sample and the diffusional properties of the reaction species. Our studies of films of polymers containing iron chloride showed that these could be converted to iron oxide in about 2 h for an 80 $\mu$m film (Fig. 18). It is reasonable to assume that the reaction time will depend roughly on the square of the thickness. Times would become very long for large pieces of material. Biological mineralization processes are characterized by time scales of months rather than minutes.

There is a limitation on the level of mineral that can be incorporated into a polymer by a simple reaction process. Most reactions that we have studied have involved reduction or hydrolysis of a compound to remove some part of the structure. As a result the final volume-loading of the composite is normally considerably less than that of the unreacted film. For instance, a 40 vol % loading of titanium tetraisopropoxide in a film results in a 4 vol % loading of titania particles. In biological composites loadings reach 90 vol % or more, but this is achieved by precipitation on a moving front rather than homogeneously within the sample (Fig. 14). Large amounts of precipitate can be incorporated, with polymer, into a solution that is then dried. Direct, controlled precipitation from a glassy polymer is more difficult, as it requires a high solubility of the solute in the polymer at elevated temperature and much lower solubility at room temperature to allow crystallization. By analogy with the glass–ceramics a high glass transition

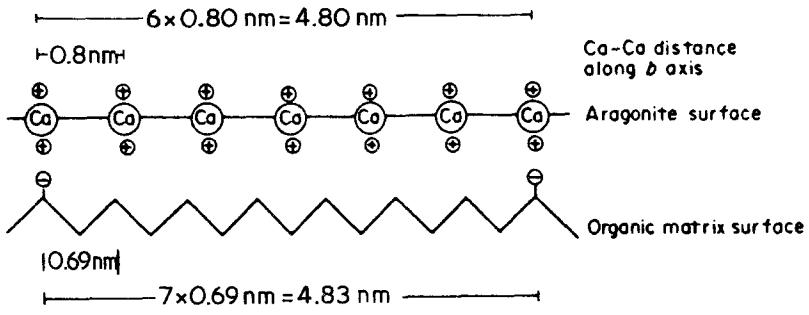


*Figure 17* Schematic representation of the possible commensurate nature of the *b* axes of aragonite and a negatively charged $\beta$-pleated sheet over a repeat distance of 4.8 nm. After Watabe [92].

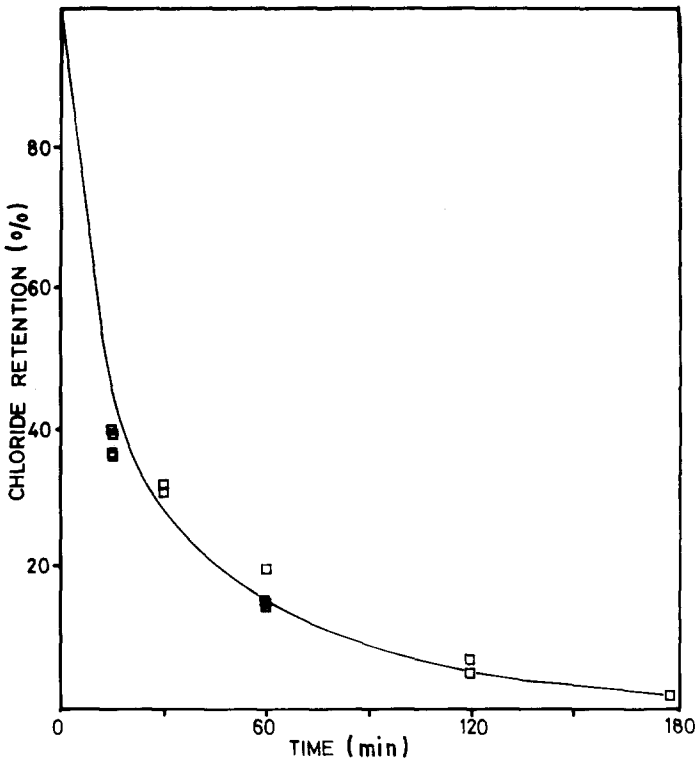


*Figure 18* Hydrolysis reaction of iron chloride solution in poly(methylmethacrylate) as measured by chloride loss from the film.

temperature for the solution would be needed, if very fine-scale precipitates were desirable. The eutectic systems would seem to offer a route to high loadings of aligned and finely divided second phases in polymers, but the miscibility of polyolefins with solutes is limited and few other systems have been investigated.

Control of precipitate orientation has been achieved in eutectics by directional solidification and, in glass–ceramics, also by extrusion. In general, our systems have involved randomly oriented and dispersed precipitates. A much higher level of morphological control is possible since biological systems can show some very complex structures. The composites of conducting organics in polymers which show high conductivities at low loadings [32] illustrate how special effects may be achieved by morphological control.

Thus, it is possible to produce many types of precipitate within a polymer matrix and, at least for thin films and fibres, these composites can be produced rapidly. Few of these materials have yet been produced with very high levels of precipitate or with oriented precipitates, but these seem quite feasible. A much more sophisticated approach would be needed to produce the very highly organized structures seen in some biological systems. In the context of biomineralization, it has been postulated that polymer membranes can be modified to give site-specific nucleation, epitaxy and orientation control. Natural systems are so complicated that it is very hard to unequivocally demonstrate these effects. To clarify these issues and explore the full range of possibilities a programme of work is needed to produce localized structured nucleation sites on polymer surfaces or in polymer gels. Interesting optical effects such as seen in opal and pearl should be possible as well as unusual electrical and transport properties.

## References


1. S. WEINER, *CRC Crit. Rev. Biochem.* **20** (1986) 365.
2. S. MANN, *Struc. Bonding* **54** (1983) 125.
3. B. D. MOYLE, R. E. ELLUL and P. D. CALVERT, *J. Mater. Sci. Lett* **6** (1987) 167.
4. J. R. JOSEPH, J. L. KARDOS and L. E. NIELSEN, *J. Appl. Polymer Sci.* **12** (1968) 1151.
5. J. L. KARDOS, W. L. McDONNELL and J. RAISONI, *J. Macromol. Sci. Phys.* **B6** (1972) 397.
6. A. SIEGMANN, M. NARKIS, M. PUTERMAN and A. T. BENEDETTO, *Polymer* **20** (1979) 89.
7. M. NARKIS, A. SIEGMANN, M. PUTERMAN and A. T. DiBENEDETTO, *J. Polym. Sci. Phys.* **17** (1979) 225.
8. A. SIEGMANN, M. NARKIS and A. DAGAN, *Polymer* **15** (1974) 499.
9. M. NARKIS, A. SIEGMANN, A. DAGAN and A. T. DiBENEDETTO, *J. Appl. Polym. Sci.* **21** (1977) 989.
10. M. J. HANNON and K. F. WISSBRUN, *J. Polym. Sci. Phys.* **13** (1975) 113.
11. A. I. KITAIGORODSKY, "Mixed Crystals", Springer Solid State Sciences Vol. 33 (Springer, Berlin, 1984).
12. P. SMITH and A. J. PENNINGS, *Polymer* **15** (1974) 413.
13. *Idem, J. Polym. Sci. Phys.* **15** (1977) 523.
14. J. C. WITTMAN and R. St J. MANLEY, *ibid.* **15** (1977) 1089.
15. J-C. ROSSO, R. GUIEU and L. CARBONNEL, *Bull. Soc. Chim. France* (1972) 934.
16. L. CARBONNEL, J-C. ROSSO and C. PONGE, *ibid.* (1972) 941.
17. R. GUIEU, C. PONGE, J-C. ROSSO and L. CARBONNEL, *ibid.* (1973) 2776.
18. R. M. MYASNIKOVA, E. F. TITOVA and E. S. OBOLONKOVA, *Polymer* **21** (1980) 403.
19. J. D. HUNT and K. A. JACKSON, *Trans. Met. Soc. AIME* **236** (1966) 843.
20. K. A. JACKSON and J. D. HUNT, *ibid.* **236** (1966) 1129.
21. H. D. KEITH and F. J. PADDEN, *J. Appl. Phys.* **35** (1964) 1270.
22. *Idem, ibid.* **35** (1964) 1286.
23. T. G. RYAN and P. D. CALVERT, *Polymer* **23** (1982) 877.

24. C. NAKAFUKU, *Polym. J.* **17** (1985) 869.
25. E. P. CHANG, *J. Appl. Polym. Sci.* **21** (1977) 937.
26. R. E. WETTON, D. B. JAMES and F. P. WARNER, *Amer. Chem. Soc. Adv. Chem.* **187** (1980) 253.
27. M. WATANABE, S. OOHASHI, K. SANUI, N. OGATA, T. KOBAYASHI and Z. OHTAKI, *Macromolecules* **18** (1985) 1945.
28. M. B. ARMAND, *Ann. Rev. Mater. Sci.* **16** (1986) 245.
29. B. VALENTI, E. BIANCHI, G. GREPPI, A. TEALDI and A. CIFERRI, *J. Phys. Chem.* **77** (1973) 389.
30. M. A. MOSKVINA, A. V. VOLKOV, T. YeGROKHOVSKAYA, A. L. VOLYNSKII and N. F. BAKEYEV, *Polym. Sci. USSR* **26** (1984) 2648.
31. J. K. JESKA, J. ULANSKI and M. KRYSZEWSKI, *Nature* **289** (1981) 390.
32. O-K. KIM, *Amer. Chem. Soc. Symp.* **242** (1984) 515.
33. J. HOCKER, F. JONAS and H-K. MULLER, *Angew. Makromol. Chem.* **145/6** (1986) 191.
34. W. J. DULMAGE, W. A. LIGHT, S. J. MARINO, C. D. SALZBERG, D. L. SMITH and W. J. STAUDENMAYER, *J. Appl. Phys.* **49** (1978) 5543.
35. J. H. PERLSTEIN, in "Electrical Properties of Polymers", edited by D. Seanor (Academic, New York, 1982) p. 59.
36. C. A. SOBON, H. K. BOWEN, A. BROAD and P. D. CALVERT, *J. Mater. Sci. Lett.* **6** (1987) 901.
37. J. E. MARK, C-Y. JIANG and M-Y. TANG, *Macromolecules* **17** (1984) 2613.
38. J. E. MARK, Y-P. NING, C-Y. JIANG, M-Y. TANG and W. C. ROTH, *Polymer* **26** (1985) 2069.
39. J. E. MARK and G. S. SUR, *Polym. Bull.* **14** (1985) 325.
40. G. S. SUR and J. E. MARK, *Eur. Polym. J.* **12** (1985) 1051.
41. S.-B. WANG and J. E. MARK, *Polym. Bull.* **17** (1987) 271.
42. P. H. HESS and P. H. PARKER, *J. Appl. Polym. Sci.* **10** (1966) 1915.
43. R. TANNENBAUM, C. L. FLENNIKEN and E. P. GOLDBERG, *J. Polym. Sci. B (Phys)* **25** (1987) 1341.
44. T. W. SMITH and D. WYCHICK, *J. Phys. Chem.* **84** (1980) 1621.
45. S. REICH and E. P. GOLDBERG, *J. Polym. Sci. Phys. Edn* **21** (1983) 869.
46. F. GALEMBECK, C. C. GHIZONI, C. A. RIBEIRO, H. VARGAS and L. C. M. MIRANDA, *J. Appl. Polymer Sci.* **25** (1980) 1427.
47. A. F. RUBIRA, A. C. Da COSTA, F. GALEMBECK, N. F. L. ESCOBAR, E. C. Da SILVA and H. VARGAS, *Colloids and Surfaces* **15** (1985) 63.
48. S. MANN, A. J. SKARNULIS and R. J. P. WILLIAMS, *J. Chem. Soc. Chem. Commun.* (1979) 1067.
49. *Idem, ibid.* (1980) 634.
50. G. J. KOVACS and P. S. VINCETT, *Can. J. Chem.* **63** (1985) 196.
51. *Idem, Thin Solid Films* **100** (1983) 341.
52. *Idem, ibid.* **111** (1984) 65.
53. D. SHUTTLEWORTH, *J. Phys. Chem.* **84** (1980) 1629.
54. J. H. LUPINSKI, *J. Appl. Polym. Sci.* **17** (1973) 1889.
55. M. NARKIS, J. YACUBOWICZ, A. VAXMAN and A. MARMUR, *Polym. Eng. Sci.* **26** (1986) 139.
56. J. D. RANCOURT and L. T. TAYLOR, *Macromolecules* **20** (1987) 790.
57. A. K. St CLAIR, V. C. CARVER, L. T. TAYLOR and T. A. FURTSCH, *J. Amer. Chem. Soc.* **102** (1980) 876.
58. T. L. WOHLFORD, J. SCHAFF, L. T. TAYLOR, A. K. St CLAIR, T. A. FURTSCH and E. KHOR, in "Conductive Polymers" edited by R. B. Seymour (Plenum, New York, 1981) pp. 7–22.
59. A. AUERBACH, *J. Electrochem. Soc.* **131** (1984) 937.
60. D. MADELEINE, S. SPILLANE and L. T. TAYLOR, *Polym. Prep* **26** (1) (1985) 92.
61. A. AUERBACH, *J. Electrochem. Soc.* **132** (1985) 1438.
62. T. YAMAMOTO, E. KUBOTA, A. TANIGUCHI, M. KUBOTA and Y. TOMINAGA, *J. Mater. Sci. Lett.* **5** (1986) 132.
63. L. E. MANRING and S. MAZUR, *J. Phys. Chem.* **90** (1986) 3261.
64. L. E. MANRING, *Polym. Commun.* **28** (1987) 68.
65. J. van WONTERGHEM, S. MORUP, C. J. W. KOCH, S. W. CHARLES and S. WELLS, *Nature* **322** (1986) 622.
66. H. HIRAI, H. WAKABAYASHI and M. KOMIYAMA, *Bull. Chem. Soc. Jpn* **59** (1986) 367.
67. H. HIRAI, *Makromol. Chemie Suppl.* **14** (1985) 55.
68. E. FITZGERALD, K. F. GADD, S. MORTIMORE and W. MURRAY, *J. Chem. Soc. Chem. Commun.* (1986) 1588.
69. Z. STRNAD, "Glass–Ceramic Materials", Glass Science and Technology, Vol. 8 (Elsevier, Amsterdam, 1986).
70. F. M. A. CARPAY and W. A. CENSE, *J. Crystal Growth* **24/25** (1974) 551.
71. W. ALBERS, *Acta Electronica* **17** (1974) 75.
72. G. KISS, *Polym. Eng. Sci.* **27** (1987) 410.
73. K. H. HENISCH, "Crystal Growth in Gels" (Penn State Press, University Park, Pennsylvania, 1970).
74. J. ABDULLAH, T. BAIRD and P. S. BRATERMAN, *J. Chem. Soc. Chem. Commun.* (1986) 256.
75. J. D. BIRCHALL and R. J. DAVEY, *J. Crystal Growth* **54** (1981) 323.
76. L. ADDADI and S. WEINER, *Proc. Nat. Acad. Sci. USA* **82** (1985) 4110.
77. A. P. WHEELER, J. W. GEORGE and C. A. EVANS, *Science* **212** (1981) 1397.
78. C. A. KNIGHT, A. L. DeVRIES and L. D. OOLMAN, *Nature* **308** (1984) 295.
79. K. M. TOWE and H. A. LOWENSTAM, *J. Ultrastruc. Res.* **17** (1967) 1.
80. R. G. BOARD, H. R. PERROTT, G. LOVE and V. D. SCOTT, *J. Zool. Lond.* **203** (1984) 329.
81. H. SILYN-ROBERTS and R. M. SHARP, *Proc. R. Soc.* **227** (1986) 303.
82. B. E. VOLCANI and T. L. SIMPSON, "Silicon and Siliceous Structures in Biological Systems" (Springer, Heidelberg, 1981).
83. M. OKAZAKI and S. SETOGUCHI, in "Origin, evolution and modern aspects of biomineralization in plants and animals", edited by R. E. Crick (Plenum, New York, in press).
84. S. MANN and C. C. PERRY, in "Silicon Biochemistry", Ciba Foundation Symposium 121 (Wiley, Chichester, 1986) p. 40.
85. H. NAKAHARA, in "Biomineralization and Biological Metal Accumulation", edited by P. Westbroek and E. W. de Jong (Reidel, Dortrecht, 1983) p. 225.
86. S. WEINER and W. TRAUB, *FEBS Lett.* **111** (1980) 311.
87. E. T. DEGENS, D. W. SPENCER and R. H. PARKER, *Comp. Biochem. Physiol.* **20** (1967) 553.
88. P. E. HARE, *Science* **139** (1963) 216.
89. S. WEINER, *Amer. Zool.* **24** (1984) 945.
90. V. R. MEENAKSHI, P. E. HARE and K. M. WILBUR, *Comp. Biochem. Physiol.* **40B** (1971) 1037.
91. S. WEINER, Y. TALMON and W. TRAUB, *Int. J. Biol. Macromol.* **5** (1983) 325.
92. N. WATABE, *Prog. Crystal Growth Charact.* **4** (1981) 99.
93. S. WEINER, *Phil. Trans. R. Soc. Lond.* **B304** (1984) 425.
94. R. E. NEWNHAM, *Ann. Rev. Mater. Sci.* **16** (1986) 47.
95. S. V. S. PRASAD and V. SITAKARA RAO, *J. Mater. Sci.* **19** (1984) 3266.

*Received 28 August*
*and accepted 5 October 1987*